LA-UR-18-21550

Title: Possible reason for the numerical value of the fine-structure constant

Author(s):   Lestone, John Paul

Intended for: Send to non-LANL people for technical review
               Web

Issued: 2018-02-27

Possible reason for the numerical value of the fine-structure constant

J. P. Lestone
Computational Physics Division, Los Alamos National Laboratory
Los Alamos, NM 87545, USA
February 21th, 2018

Abstract

A simple picture of the electron emerges if there is a cross section of $\pi\lambdabar^2$ for vacuum virtual photons to stimulate an isolated electron to emit an additional virtual photon. This reaction mechanism leads to the storage of the rest-mass energy in the surrounding cloud of virtual photons. The Lamb shift can be obtained if one out of every $1/\alpha$ of the stimulated emissions is preceded by the absorption and re-emission of the incident vacuum virtual photon including the corresponding electron recoil. This suggests a "doorway" cross section of $\alpha\pi\lambdabar^2$ plays a key role in some QED processes. Additional support for this suggestion is obtained via a simple semi-classical picture of Compton scattering. Several speculative semi-classical reaction mechanism choices, including near-field effects, give the anomalous magnetic moment of the free electron. These choices are partially justified by their ability to give the magnetic moment of electrons in hydrogen-like atoms as a function of the atomic number of the corresponding nucleus, close to the correct result. The stimulated-emission process used to obtain the rest-mass energy allows for the possibility that stimulated virtual photons can be exchanged between an electron pair. This exchange can be used to estimate a repulsive force between electrons, and thus allows for a calculation of the fine-structure constant. A result near to the experimental value is obtained with minor modifications to the assumptions that give the rest mass, Lamb shift, and anomalous magnetic moment of the electron. Additional studies are required to confirm or negate the suggestions made here.

I.   Introduction

Quantum electrodynamics (QED) is one of the most successful and tested theories ever developed, and can be viewed as one of the pinnacles of human thought. Unfortunately, a full and detailed understanding requires both talent and a significant time commitment. QED's development was not easy and it took several decades of concerted effort by many authors to obtain a working theory capable of giving precise predictions. The first steps to a usable theory of the interaction of matter and light, consistent with both special relativity and quantum mechanics, were taken by Dirac in the late 1920s [DIR27]. Significant contributions by others followed, culminating in a series of papers by Tomonaga [TOM46], Schwinger [SCH48], Feynman [FEY49], and Dyson [DYS49]. Those trained in QED have since been able to calculate many experimental observables with extraordinary precision. However, precise manual calculations require monumental effort, and are not amenable to a lone physicist with a casual interest in QED. For example, the anomalous magnetic moment of the electron, $(g-2)/2$, was not obtained to fourth- and sixth-order until 1957 [PET57] and 1996 [LAP96], respectively. The theoretical relationship between $(g-2)/2$ and the fine-structure constant, α, is now known to tenth-order [KIN06,

AOY07, AOY12], and considered to be so strong and the modern $(g–2)/2$ measurements so precise [GAB06], that the modern estimate of α = 1/137.0359991 [MOH15] is inferred from the $(g–2)/2$ measurements via QED theory.

The aim of the present study is to find a series of relatively simple semi-classical assumptions and/or reaction mechanisms that can be used to calculate several QED based phenomena without the use of full quantum theory or detailed special relativity. We will not necessarily attempt a detailed justification of all the assumptions, but only note that thinking a certain way leads to computational results that are close to experimental observations. Many of these assumptions may appear unorthodox to those who are experts in QED, but perhaps resonate with those looking for a simple way of obtaining a more intuitive feel of some QED processes without the investment in time required to obtain a full understanding. To be clear, the reader should be aware that the semi-classical reaction mechanisms presented here are reverse engineered from the known experimental results, and are no substitute for full quantum field theory calculations, which form the cornerstone of our understanding of elementary particles and fields. However, the approaches used here to obtain simple methods for a partial understanding of some QED processes lead to an explanation for the size of the repulsive force between two electrons, and thus to a reason for the numerical value of the fine-structure constant.

II. Vacuum virtual photon electron interaction cross section

The central theme of this manuscript is the consideration of the possibility that there is a fundamental photon-electron interaction cross section at the heart of several QED processes. The size and the consequences (outcomes) of this cross section can the examined by calculating observable outcomes from various hypotheses, and comparing to the corresponding experimental results. To limit the number of considered properties of the above-mentioned photon-electron interaction, existing well-known theory can be used as a guide. For example, the interaction cross section (particularly for nuclear reactions) between spherically symmetric projectiles and targets can be written as

$$\sigma(\varepsilon) = \sum_{L=0}^{\infty} T_L(\varepsilon)\pi\lambdabar^2, \tag{II.1}$$

where $\lambdabar$ is the reduced wavelength of the projectile-target system, and the $T_L(\varepsilon)$ are orbital angular momentum and energy-dependent transmission coefficients. In the limit of very small point-like objects (without long-range forces), an interaction can only proceed via "central" collisions with no relative orbital angular momentum between the projectile and target. This is why low-energy neutron-induced reactions proceed via the $L=0$ incoming s wave with minimal contributions via the $L=1$ p wave. For the photon-electron interaction, our first assumption is:

A1 $T_{L=0}(\varepsilon) = 1$ for ε less than a high-energy cutoff ε_H, and zero for all $L\neq 0$, i.e. an interaction cross section of $\pi\lambdabar^2$.

A cross section does not only have a size but must also have a consequence; for example, a fusion or fission cross section in nuclear physics. The description of the consequence associated with A1 is our second assumption:

A2 The electron is stimulated to emit an additional virtual photon (a stimulated virtual photon), while the incident vacuum virtual photon proceeds on as if nothing has happened.

The direction of the simulated emission is not necessarily the same as the incident photon, because the effective size of the emitter is the same "size" as the emitted photon (as per A1). This is analogous to the Hanbury Brown and Twiss effect [HAN56] where correlated photons emitted from a finite size object are not emitted parallel, but with typical angles between the correlated photons of ~ $\lambdabar$ divided by the

radius of the emitter. Here, the effective size of the emitter/absorber is λ, as per A1. The stimulated emission of a virtual photon by the passage of the nearby vacuum virtual photon is depicted in Fig. II.1 (and later in Fig. II.2).
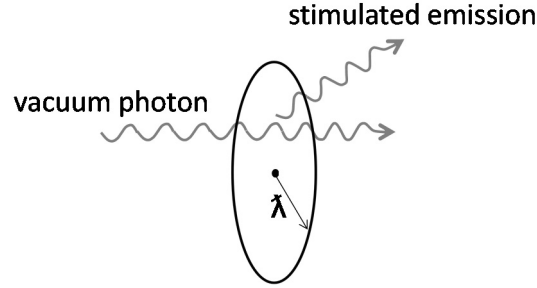

Fig. II.1. Depiction of a stimulated virtual emission generated by the passage of the vacuum virtual photon within λ of a point particle. The wavelength of the schematic photons is not to scale.

Of course, the stimulated emission from a fixed-mass object like an electron violates conservation of energy and momentum, and would not be allowed if only classical physics is assumed. However, the emission is allowed for a time scale of $\tau \sim \hbar/(2\varepsilon)$ via the time-energy uncertainty principle, and thus we invoke:

   A3   For an isolated electron, the stimulated emission from A2 travels away from the electron at the speed of light c and "disappears" on a time scale of $\hbar/(2\varepsilon)$.

This gives an exponential distribution of the semi-classical survival times, $P(t) \propto \exp(-2t\varepsilon/\hbar)$, with the stimulated virtual photons travelling approximately one-half their wave length before "disappearing." A3 will be modified later with the addition of self-absorption, and the absorption by a neighboring particle as other methods by which the stimulated photon can end its life.

   The high-energy cutoff introduced in A1 can be estimated via a variety of thought experiments. For example, thinking semi-classically, photons can interact fully with (i.e. shake) an isolated charged electron when the wavelength is much larger than an electron's effective size. If the wavelength of an incident electromagnetic wave becomes smaller than an electron's effective size then different parts of the high-frequency wave "try" to push different parts of the electron in opposite directions, and thus the overall strength of the total interaction (shaking) decreases. Setting the wavelength of the high-energy cutoff to the reduced Compton wavelength $\lambda_C = \hbar c/(mc^2)$ gives $\varepsilon_H \sim hc/\lambda_C = 2\pi mc^2$. This logic is relatively vague, and should not be believed unless backed up by additional arguments.

II.A   Virtual-photon emission rate from an electron

   Using assumptions A1 and A2 the stimulated emission rate from an isolated electron can be determined by multiplying the production cross section by the number density of vacuum virtual photons [BJO64] by the speed of light

$$R = \int_0^{\varepsilon_H} R(\varepsilon)d\varepsilon = \int_0^{\varepsilon_H} \pi\lambda^2 \frac{\varepsilon^2 d\varepsilon}{\pi^2\hbar^3 c^3} c = \int_0^{\varepsilon_H} \frac{d\varepsilon}{\pi\hbar} = \frac{\varepsilon_H}{\pi\hbar} . \tag{II. 2}$$

Here we have assumed ε_H operates as a sharp cutoff. This sharp cutoff is likely unphysical. However, we apply the philosophy that if a simplistic approach appears to work then we shall keep it until a more sophisticated one is needed. All spontaneous emission rates can be viewed as the stimulated emission of photons induced by vacuum virtual photons, and thus Eq. (II.2) can be viewed as the spontaneous emission rate of virtual photons from an electron.

II.B   Rest-mass energy

Combining Eq. (II.2) with A3, the additional average virtual-photon energy (above the virtual-photon vacuum ground-state energy) associated with the presence of an isolated electron can be expressed as

$$\bar{E} = \int_0^{\varepsilon_H} \int_0^{\infty} \frac{\varepsilon}{\pi\hbar} \frac{t\exp(-2\varepsilon t/\hbar)\,dt}{\int_0^{\infty}\exp(-2\varepsilon t/\hbar)\,dt}\,d\varepsilon$$

$$= \int_0^{\varepsilon_H} \int_0^{\infty} \frac{2\varepsilon^2}{\pi\hbar^2} t\exp(-2\varepsilon t/\hbar)\,dt\,d\varepsilon = \frac{1}{2\pi}\int_0^{\varepsilon_H} d\varepsilon = \frac{\varepsilon_H}{2\pi} = mc^2. \quad (\text{II. }3)$$

This result supports the previous suggestion that the high-energy cutoff is $\varepsilon_H = 2\pi mc^2$. The reaction mechanism by which Eq. (II.3) gives the rest-mass energy is pictured in Fig. II.2.
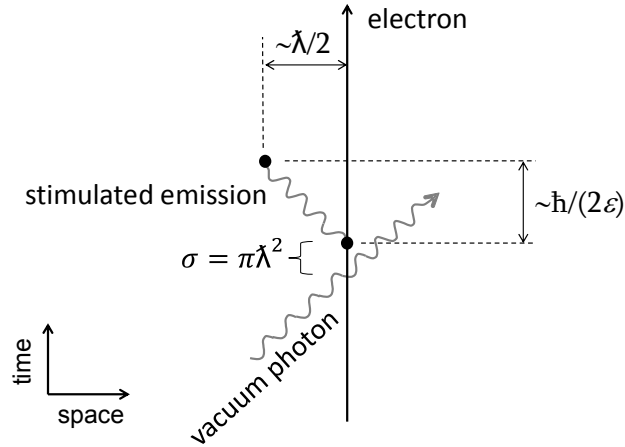

Fig. II.2. A Feynman-like diagram of the proposed mechanism by which the rest-mass energy of the electron is stored in the surrounding cloud of stimulated virtual photons generated by an interaction of the "naked" electron with the vacuum virtual photons.

The mechanism presented here does not explain the size of the electron's mass, but does give a physical mechanism for the existence of the rest mass as the energy tied up in the cloud of stimulated virtual photons surrounding an isolated charged particle. In this explanation, one could assume that the high-energy cutoff is a fundamental quantity, and this leads to a mass equal to the reduced cutoff energy which, in turn, leads to an effective size consistent with the assumed cutoff. This interpretation has no problem with point-like particles, unlike the storage of the rest mass in the electric field surrounding a classical point particle. The concept of the particle's mass being contained in a surrounding cloud of virtual photons easily gives the relativistic mass of a particle as a function of its velocity because of the different rates of the passage of time between different inertial frames that control the time-energy uncertainty principle. The Doppler shift of the virtual photons associated with an electron's velocity also gives the result that an electron's momentum is stored in the surrounding cloud of virtual photons (a simple exercise for the reader).

A simple semi-classical picture of why charged particles can "erupt" from the vacuum for a short time period is also obtained. This is because of the interpretation that the rest-mass energy is stored in the surrounding cloud of stimulated virtual photons, and not in the point-like particle in the middle of the cloud. If a naked point-like electron is born at time t=0 (without its cloud of stimulated virtual photons) it will take a finite time scale for the first vacuum virtual photon to find the new electron. This time scale

is the inverse of the rate given by Eq (II.2) and is equal to $\pi\hbar/\varepsilon_H = \hbar/(2mc^2)$, in agreement with the time-energy uncertainty principle. This is not surprising, because the time-energy uncertainty principle is inputted via A3. What is of interest is that a simple semi-classical picture emerges, and that this picture is only self-consistent with the time-energy uncertainty principle if the high-energy cutoff is $\varepsilon_H = 2\pi mc^2$.

The results obtained thus far suggest that naked electrons have no intrinsic mass; the electron's mass is defined by a finite high-energy cutoff in the photon naked-electron cross section of $2\pi mc^2$, where m is the electron mass; the average energy stored in the surrounding cloud of stimulated virtual photons is mc^2; and it takes a time scale of $\hbar/(2mc^2)$ after the birth of a naked electron for a vacuum virtual photon to find the electron and generate the first rest-mass storing stimulated virtual photon.

II.C   Black-body emission

The spontaneous-photon emission rate from a spherical black-body can be obtained via transition state theory, with the emission rate of uncorrelated photons from a large black-body sphere [LES08]

$$R = \frac{2}{2\pi\hbar} \int_0^\infty \sum_{L=0}^{L_{max}} (2L + 1) \exp(-\varepsilon/T) \, d\varepsilon. \tag{II.4}$$

The maximum angular momentum that a photon can carry away from a macroscopic sphere of radius r is $L_{max}\hbar = r\varepsilon/c$. Substituting into Eq. (II.4), and taking the limit of a large macroscopic object, gives the spontaneous black-body emission rate (excluding the amplification associated with stimulated emission in the object's surface) [LES08]

$$R = \frac{4\pi r^2}{4\pi^2\hbar^3 c^2} \int_0^\infty \varepsilon^2 \exp(-\varepsilon/T) \, d\varepsilon. \tag{II.5}$$

In the limit of a very small object, only $L=0$ emission and/or absorption is allowed, and the spontaneous emission rate becomes

$$R = \frac{1}{\pi\hbar} \int_0^\infty \exp(-\varepsilon/T) \, d\varepsilon. \tag{II.6}$$

In the limit of an infinitely hot object, this rate becomes

$$R = \frac{1}{\pi\hbar} \int_0^{\varepsilon_H} d\varepsilon = \frac{\varepsilon_H}{\pi\hbar}. \tag{II.7}$$

This result is the same as Eq. (II.2), and suggests A1 and A2 are the same as assuming electrons behaving like very small and very hot black bodies. This, in turn, suggests electrons resemble virtual-photon Hawking-radiating micro black holes. As previously discussed, the emission represented by Eq. (II.7) violates conservation of energy and momentum if from a fixed-mass object like an electron, and is not allowed if only classical physics is assumed. However, if in a time scale of $\sim\hbar/(2\varepsilon)$ a stimulated virtual photon were to re-establish the appropriate conservation rules by being absorbed by a nearby partner electron, then the exchange of virtual photons between two electrons would be allowed. The rest of this manuscript is an attempt to provide support for the idea that the above-discussed exchange mechanism might be the cause of the electromagnetic repulsion between two electrons. This force can be used to estimate the numerical value of the fine-structure constant. Before calculating the fine-structure constant, we determine other details that appear important to an understanding of virtual-photon electron interactions by studying the Lamb shift, Compton scattering, and the magnetic moment of electrons in the next three sections.

III. Hydrogen Lamb shift

According to the Dirac equation (without including vacuum physics), the hydrogen $2s_{1/2}$ and $2p_{1/2}$ levels should be degenerate (have the same energy). This is a consequence of an assumed pure inverse-square-law Coulomb force between the electron and the proton. There are many reasons why the true interaction will not follow a perfect inverse-square law at small distances. These include the finite size of the proton, vacuum polarization associated with virtual electron-positron pairs [UEH35], and a possible intrinsic fuzziness of the electromagnetic interaction involving electrons on small length scales. In 1947 Lamb and Retherford [LAM47], using microwaves, demonstrated that the hydrogen $2s_{1/2}$ level sits ~1000 MHz above the $2p_{1/2}$ level. Bethe showed in the same year [BET47] that this observation was predominantly due to the electromagnetic vacuum interacting with the electron. A more modern measurement of the Lamb shift is 1057.85 MHz [KAR98]. The corresponding QED calculations [KAR98] are consistent with experiment.

Welton [WEL48, BJO64] obtained a simple qualitative description of the Lamb shift by invoking a semi-classical model of the time dependence of the electric field of the vacuum state, and how these fluctuations smear out the location of an electron. The corresponding root-mean-square (rms) spread in the electron's location associated with its interaction with the vacuum is [BJO64, pg. 60]

$$\delta r^2 = \frac{2\alpha \lambdabar_C^2}{\pi} \int \frac{d\varepsilon}{\varepsilon}. \tag{III.1}$$

The integral in Eq. (III.1) is over the energy of the virtual photons, and diverges if the lower limit is zero and/or if the upper limit is infinite. Therefore, in order to obtain a finite result, there need to be both low- and high-energy cutoffs. A possible value for the high-energy cutoff is discussed above ($\varepsilon_H = 2\pi m c^2$). For a bound electron, there must be a low-energy cutoff, because wavelengths very much larger than the characteristic size of the system (approximately the Bohr radius) cannot shake the bound-electron independent of the proton. Here, we assume the Lamb shift low-energy cutoff is the energy of a photon with a wavelength equal to one-half the Bohr circumference, i.e. $\varepsilon_L = \alpha m c^2 / \pi$.

From the Darwin term in the Dirac equation it follows that the hydrogen Lamb shift is [BJO64, pg. 59]

$$\Delta E_n = \frac{2\pi}{3} \alpha \hbar c \; \delta r^2 \; |\psi_n(0)|^2. \tag{III.2}$$

For those not familiar with the Dirac equation, this derivation is not very transparent, so we also show a derivation of Eq. (III.2) using first-order perturbation theory where the shift in the energy of a given state is

$$\Delta E = \int \psi \, \Delta V \, \psi^* dv, \tag{III.3}$$

where ΔV is the perturbation of the potential. Invoking the central-limit theorem and the large number of randomly orientated and phased vacuum modes, the blurriness of an electron's charge associated with its interaction with the electromagnetic vacuum will be Gaussian with a variance of δr^2 [see Eq. (III.1)]. The size of the Lamb shift can be shown to depend only on the rms spread of the electron's blurriness, and not on the details of the shape of the distribution (an exercise for the reader). Given this, we chose the simplest distribution of a delta spike at a radius of δr to evaluate the Lamb shift. This choice causes ΔV to be zero for $r > \delta r$ and $\Delta V = \alpha \hbar c (1/r - 1/\delta r)$ for $r < \delta r$, and enables us to write the shift in a hydrogen level as

$$\Delta E = \int_0^{\delta r} |\psi(r)|^2 \alpha \hbar c \left(\frac{1}{r} - \frac{1}{\delta r} \right) 4\pi r^2 \, dr. \tag{III.4}$$

Given that $\delta r \ll \lambdabar_C/\alpha$ (the characteristic length scale of hydrogen), the radial dependences of the *s* wave function can be set constant over the range of the integral in Eq. (III.4) giving

$$\Delta E_{ns} = 4\pi\alpha\hbar c |\psi_{ns}(0)|^2 \int_0^{\delta r} \left(r - \frac{r^2}{\delta r} \right) dr = \frac{2\pi}{3} \alpha\hbar c \, \delta r^2 \, |\psi_{ns}(0)|^2, \qquad (\text{III}.5)$$

in agreement with Eq. (III.2).

If we apply the low- and high-energy cutoffs of $\alpha mc^2/\pi$ and $2\pi mc^2$ to Eq. (III.1) then

$$\delta r^2 = \frac{2\alpha\lambdabar_C^2}{\pi} \int_{\alpha/\pi}^{2\pi} \frac{d\varepsilon}{\varepsilon} = \frac{2\alpha \ln(2\pi^2/\alpha)\lambdabar_C^2}{\pi} \quad \text{and} \quad \Delta E_{2s} = \frac{\alpha^5 \ln(2\pi^2/\alpha)}{6\pi} mc^2 = 1072 \text{ MHz}. \quad (\text{III}.6)$$

Correcting for the shift in the 2*s* level associated with the polarization of the vacuum [UEH35] (−27 MHz), the shift in the $2p_{1/2}$ level [BET50, KAR52] by −13 MHz, and the small correction due to the proton's size [KEM33] (<0.2 MHz) gives a final estimate of the hydrogen Lamb shift of 1058 MHz. Given the approximations made, the level of agreement with experiment is stunning, but possibly fortuitous. However, the success of Eq. (III.6) may be due to the more prudent choice of cutoff energies, and the fact that simple semi-classical methods sometimes give accurate results as demonstrated by the Bohr theory of the hydrogen atom.

Here, we introduce a new method for obtaining Eq. (III.1) by invoking a semi-classical photon (particle) picture of the electromagnetic vacuum. To obtain Eq. (III.1) in a semi-classical photon picture of the electromagnetic vacuum, we assume that stimulated emission is not the only consequence of the $\pi\lambdabar^2$ interaction cross section introduced in section II:

A4   One out of every $1/\alpha$ of the interactions from A1 involves the initial absorption of the incident photon, the recoil of the electron, and then the re-emission of the original photon, before the emission of the additional stimulated virtual photon discussed in A2 and A3. Of course, the initial absorption violates conservation of energy and momentum and is not allowed if only classical physics is assumed. However, by invoking the time-energy uncertainty principle we allow the absorption to occur, as long as the absorbed photon is re-emitted back into its original state on a time scale given by $\tau \sim \hbar/\varepsilon$ (see Fig. III.1). Notice that here we have allowed a time scale of $\sim\hbar/(2\varepsilon)$, for each of the absorption and emission processes.

Given the above assumptions, the rate that vacuum virtual photons are absorbed (and then re-emitted) by an isolated electron can be obtained by multiplying Eq. (II.2) by α, giving

$$R_a(\varepsilon) = \alpha\pi\lambdabar^2 \frac{\varepsilon^2 d\varepsilon}{\pi^2\hbar^3 c^3} c = \frac{\alpha d\varepsilon}{\pi\hbar}. \qquad (\text{III}.7)$$

A Feynman-like diagram of the reaction mechanism used here to obtain the Lamb shift is displayed in Fig. III.1. On absorption (in the non-relativistic limit), the electron recoils with a velocity of $\varepsilon/(mc)$ and travels a distance $r \sim \varepsilon/(mc)\times\hbar/\varepsilon = \lambdabar_C$, before the absorbed photon is re-emitted. Following this re-emission we assume the electron is returned to its original pre-absorbed state. If the probability per unit time to complete both the absorption and re-emission process is assumed to be $\hbar/\varepsilon$, then there will be an exponential ensemble of recoil distances, $\exp(-r/\lambdabar_C)$, with a mean value of $\lambdabar_C$. The same result is obtained with relativistic kinetics if the time scale $\tau = \hbar/\varepsilon$ is assumed to apply in the reference frame of the recoiling particle. For a given recoil distance r, the average rms spread of the electron's location averaged along its path is $r^2/3$ (assuming a constant recoil velocity), with a recoil time of rmc/ε. Combining these effects gives an rms spread of an electron's location due to the recoils associated with the absorption and re-emission of vacuum virtual photons of

$$\delta r^2(\varepsilon) = \frac{\int_0^\infty \frac{r^2}{3}\frac{rmc}{\varepsilon}\frac{\alpha d\varepsilon}{\pi\hbar}\exp(-r/\lambdabar_C)dr}{\int_0^\infty \exp(-r/\lambdabar_C)dr} = \frac{\alpha mc^2}{3\lambdabar_C\pi\hbar c}\frac{d\varepsilon}{\varepsilon}\int_0^\infty r^3\exp\left(-\frac{r}{\lambdabar_C}\right)dr = \frac{2\alpha\lambdabar_C^2}{\pi}\frac{d\varepsilon}{\varepsilon}. \quad (\text{III.8})$$
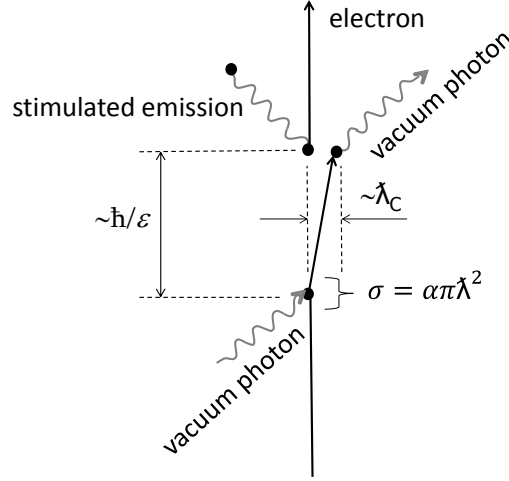
Fig. III.1. A Feynman-like diagram of the reaction mechanism used to obtain Eq. (III.8) (the Lamb shift). This diagram is the same as in Fig. II.2, except the incident vacuum virtual photon is first absorbed with a cross section of $\alpha\pi\lambdabar^2$ and re-emitted before the generation of the stimulated virtual photon. To keep the total interaction cross section of $\pi\lambdabar^2$, the recoil-less reaction cross section (A1; and see Fig. II.2) is reduced to $(1-\alpha)\pi\lambdabar^2$.

Integrating Eq. (III.8) over the energy of the relevant vacuum photons gives Eq. (III.1). This result partially justifies A4. However, an additional assumption in required for Eq. (III.8) to be the main term associated with the Lamb shift:

A5 The stimulated emission that "disappears" after a time $\tau \sim \hbar/(2\varepsilon)$ from A1-A3 does not contribute to the smearing of an electron's location, i.e. we need to assume that the stimulated emission that generates the rest mass is only felt though an average integrated over all emission directions.

Perhaps this is caused by the lack of a termination site at a real particle position, and thus spherical symmetry is not broken (in an inertial frame).

The apparent success in obtaining a simple method by which the Lamb shift can be understood suggests a "doorway" cross section of $\alpha\pi\lambdabar^2$ plays a key role in some QED processes. To test this hypothesis, we attempt to obtain a simple understanding of Compton scattering in the next section.

IV. Compton scattering

The $\alpha\pi\lambdabar^2$ absorption cross section used in section III can be thought of as a first step (a doorway cross section) in the process of Compton scattering. First, the electron makes an attempt to absorb the incident photon with a cross section $\alpha\pi\lambdabar^2$. If no other steps occur, this attempted absorption must fail as in section III, with the re-emission of the incident photon. In the second step, the electron is assumed to recoil with velocity $v = \varepsilon/(mc)$, which it obtains over the absorption time scale $\tau = \hbar/(2\varepsilon)$. The recoil thus involves an electron acceleration of $a = 2\varepsilon^2/(\hbar mc)$ over a time period of τ. This is inconsistent with the constant and instantaneous recoil velocity assumed in section III to obtain the Lamb shift. We accept that simple semi-classical pictures of different processes may need to use different assumptions that

capture the different essences of these processes. Our picture of the Lamb shift requires acknowledgement of a recoil velocity and the corresponding displacement, but not the corresponding acceleration associated with the velocity change. Our picture of Compton scattering needs us to acknowledge the electron's acceleration associated with photon absorption, but does not require us to consider any physical spatial displacement of the electron. Perhaps these are related to the Lamb shift being an energy shift associated with electron displacements (but not accelerations), while the Compton cross section's size is related to the acceleration of the recoil (but not dependent on its displacement). An interplay between our knowledge of displacement and acceleration may be due to a combined effect of both the position-momentum, and time-energy uncertainty principles. If an acceleration exists for a time τ then conservation of energy can be violated by $\sim \hbar/(2\tau)$. Dividing the position-momentum uncertainty principle by τ gives $\Delta x \cdot m \cdot \Delta a \sim \hbar/(2\tau)$, where Δa is the uncertainty of the acceleration operating over the time interval τ. For macroscopic (long) time intervals, both displacement and acceleration can be simultaneously known to high accuracy. However, for the recoils of mass m objects associated with the absorption of individual photons with energies $<< mc^2$, the equation $\Delta x \cdot m \cdot \Delta a \sim \hbar/(2\tau)$ implies that either the corresponding displacement or the acceleration can be known accurately, but not both simultaneously.

 The power of emission from an accelerating classical charge in the non-relativistic limit is given by [JAC75]

$$P = \frac{2}{3} \frac{e^2}{4\pi\epsilon_0} \frac{a^2}{c^3} = \frac{2\alpha\hbar c a^2}{3c^3}. \tag{IV.1}$$

The electromagnetic energy emitted by the electron during the acceleration phase of the attempted absorption is therefore

$$E = \frac{2\alpha\hbar c a^2 \tau}{3c^3} = \frac{2\alpha\hbar c}{3c^3} \frac{4\varepsilon^4}{(\hbar mc)^2} \frac{\hbar}{2\varepsilon} = \frac{4\alpha}{3} \frac{\varepsilon^3}{(mc^2)^2}. \tag{IV.2}$$

In the low-energy limit, conservation of energy could be re-established by the emission of a photon of energy ε during the acceleration phase. To estimate the probability of such an emission we use:

  A6   Emission during the acceleration phase of the electron recoil manifests itself as a single photon of energy ε. The probability of emitting such an energy and momentum conservation-reestablishing real photon from an individual recoiling electron can be expressed as the total classical energy emission [see Eq. (IV.2)] divided by the energy of the required photon.

The corresponding emission probability is given by (in the non-relativistic limit)

$$P = \frac{4\alpha}{3} \frac{\varepsilon^2}{(mc^2)^2}. \tag{IV.3}$$

The initial absorption attempt can only be successful if the energy and momentum conservation-reestablishing photon emission occurs. The corresponding interaction cross section is given by

$$\sigma = P\alpha\pi\lambda^2 = \frac{4\alpha}{3} \frac{\varepsilon^2}{(mc^2)^2} \frac{\alpha\pi(\hbar c)^2}{\varepsilon^2} = \frac{4\pi\alpha^2 \lambda_C^2}{3}. \tag{IV.4}$$

The third step is to realize that Eq. (IV.4) is only half the real cross section, because in obtaining Eq. (IV.4), the photon absorption is assumed to occur before the recoil-induced photon emission. However, via the time-energy uncertainty principle, the order of these processes can be reversed, i.e. it is also possible for an isolated electron to spontaneously accelerate, emitting a photon of energy ε, in the presence of an incident real photon of energy ε, but before the absorption of the incident photon. This spontaneous acceleration and emission violates conservation of energy and momentum, but via quantum mechanics is allowed to occur on a time scale of $\tau = \hbar/(2\varepsilon)$ before the incident photon is absorbed re-

establishing conservation of energy and momentum. This is the same effect as in standard second-order QED where two Feynman diagrams are needed [BJO64, pg 128] (see Fig. IV.1) to calculate the Compton cross section. This effect doubles Eq. (IV.4), giving our final result for the Compton cross section, in the non-relativistic limit

$$\sigma_C = \frac{8\pi\alpha^2 \lambdabar_C^2}{3}. \tag{IV.5}$$

The arguments presented here are not meant to supersede or replace standard QED, but perhaps can be used to give physicists with little or no background in QED, a simplified picture which captures some essence of the Compton scattering process. The presence of such a simple picture supports the suggestion that a doorway cross section of $\alpha\pi\lambdabar^2$ plays a key role in some QED processes.
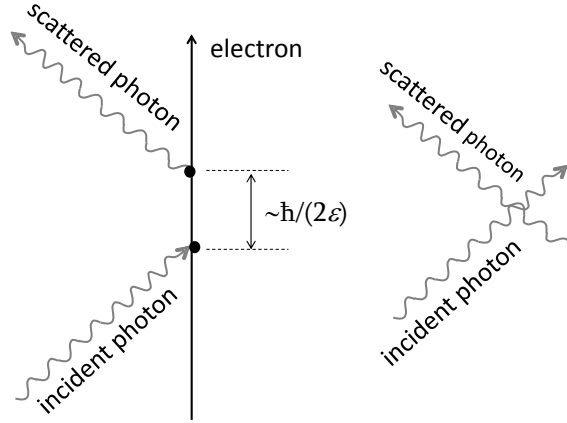

Fig. IV.1. The two second-order Compton scattering Feynman diagrams

V.   Anomalous magnetic moment of the electron

   To obtain a simple picture of the anomalous magnetic moment of a free electron, we are at first guided by the fact that the anomalous magnetic moment is caused by the emission and reabsorption of virtual photons, and introduce:

   A7   An electron can "self-absorb" its own stimulated virtual photon in a time scale of $\tau = \hbar/\varepsilon$.

As in the case of the Lamb shift, a time of $\hbar/(2\varepsilon)$ is allotted to both emission and absorption. Assuming only classical physics, the self-absorption could never occur because the stimulated emission and the corresponding recoiling electron would be heading in opposite directions. To overcome this "problem" we introduce:

   A8   The cross section for the reabsorption of a stimulated virtual photon is assumed to be $\pi\lambdabar^2$ if the distance between the birth and reabsorption locations d is very much larger than $\lambdabar$, but with a new high-energy reabsorption cutoff, $\varepsilon_R < \varepsilon_H$, that is influenced by the state of the electron. The corresponding time dependent reabsorption probability is $P(t) = \pi\lambdabar^2/(4\pi d^2)$, where d is the distance traveled by the recoiling electron with velocity $v = \varepsilon/(mc)$.

We assume the high-energy reabsorption cutoff ε_R is inversely proportional to the wavelength of the electron, and therefore quasi-free electrons in a macroscopic trap have a very small high-energy cutoff. Using A7 and A8, the probability that a given stimulated virtual photon is self-absorbed is given by

$$P_{\text{sa}} = \frac{\int_0^\infty \int_0^{\varepsilon_R} \frac{\pi\lambdabar^2}{4\pi x^2} \exp\left(\frac{-x}{\lambdabar_C}\right) dx\, d\varepsilon}{\int_0^\infty \int_0^{\varepsilon_R} \exp(-x/\lambdabar_C) dx\, d\varepsilon} = \frac{1}{\lambdabar_C \varepsilon_R} \int_0^\infty \int_0^{\varepsilon_R} \frac{\hbar^2 c^2}{4x^2 \varepsilon^2} \exp\left(\frac{-x}{\lambdabar_C}\right) dx\, d\varepsilon \; . \tag{V.1}$$

This is further simplified by switching to a length scale in units of $\lambdabar_C$ and an energy scale of mc^2, giving

$$P_{\text{sa}} = \int_0^\infty \int_0^{\varepsilon_R} \frac{1}{4x^2 \varepsilon^2} \exp(-x) \frac{dx\, d\varepsilon}{\varepsilon_R} \; . \tag{V.2}$$

This gives the unphysical result of an infinite probability due to the $1/x^2$ term. This situation can be rectified by the realization that near-field effects will introduce an effective low-energy cutoff by modifying the absorption cross section for photons "falling" towards an electron from a finite starting distance d. The reabsorption cross section of $\pi\lambdabar^2$ for $d \gg \lambdabar$, is consistent with the effective semi-classical photon-electron interaction size of $\lambdabar$ (see section II). Near-field effects should start growing rapidly as the separation decreases through $\sim 2\lambdabar$, and be strong for photons starting a distance $d < \lambdabar$, with the photons increasingly losing their ability to interact with the particle as d decreases towards zero. This gives the result that, as $d \to 0$, a photon has no time (and/or space) to be absorbed, and fails to interact with the nearby particle. In an attempt to include near-field effects we introduce:

A9 Absorption proceeds via a distribution of effective absorption/emission sites around each electron. Here, we assume this distribution of absorption sites is given by $\exp(-r^2/(2\lambdabar^2))$ (the harmonic oscillator ground-state wave function). The absorption amplitude per unit distance traveled by the photon is assumed to be proportional to the density of absorption sites. The absorption cross section for a photon starting a distance d from an electron is then given by

$$\sigma_{\text{nf}}(\lambdabar, d) = \left| \frac{2}{\lambdabar\sqrt{2\pi}} \int_0^d \exp\left(\frac{-r^2}{2\lambdabar^2}\right) dr \right|^2 \pi\lambdabar^2 = \text{erf}^2\left(\frac{d}{\lambdabar\sqrt{2}}\right) \pi\lambdabar^2 = f_{\text{nf}}\, \pi\lambdabar^2, \tag{V.3}$$

for photon energies $< \varepsilon_R$. Including A9 leads to the finite result

$$P_{sa} = \int_0^\infty \int_0^{\varepsilon_R} \text{erf}^2\left(\frac{x\varepsilon}{\sqrt{2}}\right) \exp(-x) \frac{dx\, d\varepsilon}{4x^2 \varepsilon^2 \varepsilon_R} \; . \tag{V.4}$$

For a very low-energy electron (in a large macroscopic trap), we set the cutoff energy ε_R to zero and rewrite Eq. (V.4)

$$P_{sa} = \int_0^\infty \int_0^{\varepsilon_R} \frac{4x^2 \varepsilon^2}{2\pi} \exp(-x) \frac{dx\, d\varepsilon}{4x^2 \varepsilon^2 \varepsilon_R} = \frac{1}{2\pi} \; . \tag{V.5}$$

This is reminiscent of the second-order QED value of $\alpha/(2\pi)$ for $(g-2)/2$. This result can be obtained with:

A10 If the stimulated virtual emission is terminated by a self-absorption then a magnetic moment of one Bohr magneton (μ_B), in the direction of the electron's spin, is generated for a time period of $t = \pi\hbar/\varepsilon_R$; and

A11 The magnetism generated by the emission and reabsorption of the stimulated virtual emission following the recoil and re-emission from A4 (as depicted in Fig. V.1) is in addition to the standard intrinsic magnetic moment associated with the Dirac equation. The emission and reabsorptions not following A4 are a part of the standard intrinsic magnetic moment associated with the Dirac equation (see Fig. V.2).

We have no plausibility arguments for A10 other than invoking it gives the desired results discussed below and in the next subsection. The self-absorption process responsible for the anomalous magnetic moment of the free electron is depicted in Fig. V.1. As discussed previously, the rate of stimulated virtual photon emission is $\varepsilon_H/(\pi\hbar)$. Via A8, only $\varepsilon_R/\varepsilon_H$ of this emission is available for reabsorption with only $1/(2\pi)$ of these reabsorption attempts being successful. Via A11, only one out of $1/\alpha$ of these

reabsorptions are associated with the anomalous magnetic moment of the free electron. Including A10 gives the anomalous magnetic moment of the free electron as

$$\mu_e = \frac{\varepsilon_\mathrm{H}}{\pi\hbar}\frac{\varepsilon_\mathrm{R}}{\varepsilon_\mathrm{H}}\frac{1}{2\pi}\alpha \cdot 1\mu_\mathrm{B} \cdot \frac{\pi\hbar}{\varepsilon_\mathrm{R}} = \frac{\alpha}{2\pi}\mu_\mathrm{B}\,, \tag{V.6}$$

in agreement with second-order QED. Most readers at this point will be saying, "unjustified assumptions have been made to generate the correct answer." This may be true. However, the proposed reaction mechanisms can be tested by the calculation of their additional consequences. For example, can the already stated assumptions lead to a calculated fine-structure constant? The short answer is yes, but additional assumptions are required to get a calculated result that is very close to the experimental value of 1/137.04. Before moving on to a calculation of the fine-structure constant, we test the previously discussed assumptions by using them to estimate the change in the magnetic moment associated with electrons in hydrogen-like atoms (ions) as a function of the charge of the atomic nucleus.
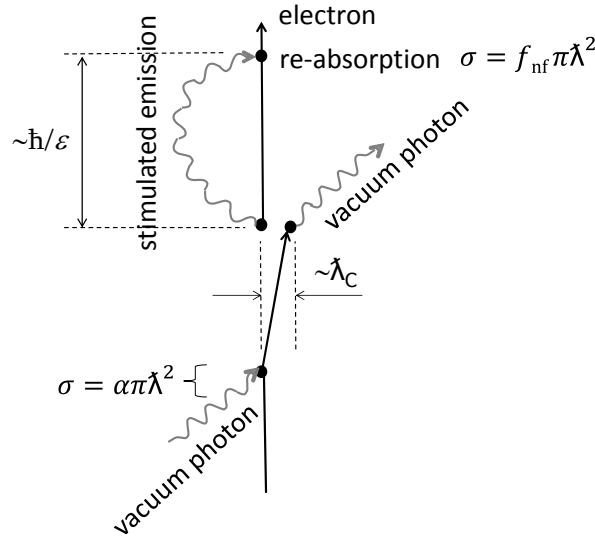

Fig. V.1. Feynman-like diagram for the reaction mechanism used here to obtain a simple representation of the anomalous magnetic moment of the free electron. This is almost the same diagram as shown in Fig. III.1. The only difference is that the stimulated virtual photon in this figure terminates on the electron.
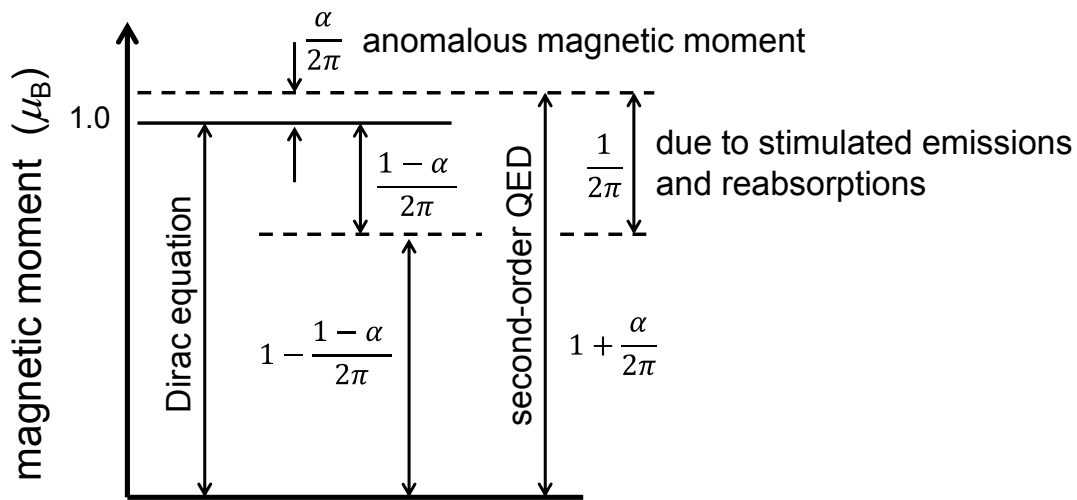

Fig. V.2. Different components of the magnetic moment of the free electron as per A11.

V.A   Magnetic moment of the electron in hydrogen-like systems

A11 appears unorthodox, and gives a breakdown of the magnetic moment of the free electron as displayed in Fig. V.2. Notice that $\mu_B/(2\pi)$ of the magnetic moment is assumed to be due to the emission and reabsorption of stimulated virtual photons. This component is divided into two parts. For free electrons, these are $\alpha\mu_B/(2\pi)$ and $(1-\alpha)\mu_B/(2\pi)$. The $\alpha\mu_B/(2\pi)$ component is associated with the emission and reabsorption following the displacement of the electron that causes the Lamb shift, and is the anomalous magnetic moment in excess of the intrinsic magnetic moment associated with the Dirac equation (see previous subsection). The $(1-\alpha)\mu_B/(2\pi)$ component is also initiated by vacuum virtual photons, but associated with interactions with no consequence on the Lamb shift, and assumed to be a part of the intrinsic magnetic moment. Both of these parts of the magnetic moment vary with the properties of the electron trap via the high-energy reabsorption cutoff, ε_R. Fig. V.3 displays the Feynman-like diagram assumed here to be the source of the dependence of the electron's magnetic moment as a function of the electron's state. This dependency on the state of the electron can be determined via Eq. (V.4).
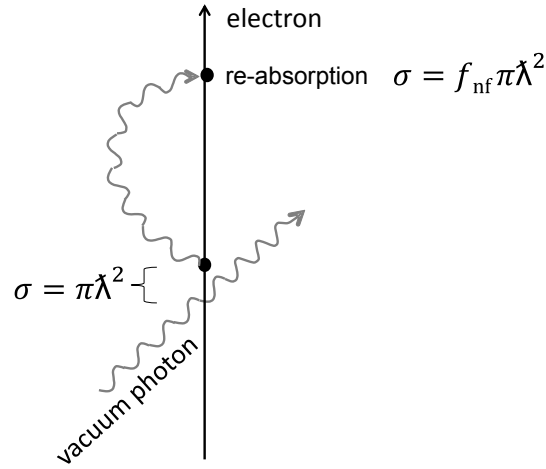

Fig. V.3. Feynman-like diagram of the reaction mechanism assumed responsible for the dependence of the electron's magnetic moment on its state. As discussed previously, the initiation cross section is separated into recoil $[\alpha\pi\lambdabar^2]$ and recoil-less $[(1-\alpha)\pi\lambdabar^2]$ components, not shown here.

The reabsorption probability of exactly $1/(2\pi)$ in Eq. (V.5) is obtained via the assumption of a large macroscopic trap and A8 and A9. Hydrogen-like atoms (ions) can be viewed as microscopic traps with a size twice the corresponding Bohr radius. Based on the discussion in the previous subsection, the size of the high-energy reabsorption cutoff will increase with the electron's momentum, and thus increase with the atomic number of the nucleus of a hydrogen-like atom. This shift in the cutoff energy to higher values decreases the calculated magnetic moment of the electron because, at higher photon energies, the error function in Eq. (V.4) becomes increasingly lower than the corresponding low-energy limit used to obtain Eq. (V.5). A reasonable representation of the electron's magnetic moment as a function of the atomic number of the nucleus in a hydrogen-like atom can be obtained by adding the assumption:

A12 The high-energy cutoff for the reabsorption cross section, ε_R, from A9 is given by the energy of a photon whose wavelength is twice the distance of the electron from the associated partner

particle, i.e. $\varepsilon_R = hc/(2d) = \pi\hbar c/d$. For electron-nucleus ground-state systems, we replace d with the corresponding Bohr radius, giving $\varepsilon_R = \alpha\pi Zmc^2$.

In reality, higher-order corrections are likely to give a reabsorption cutoff of $\varepsilon_R = \alpha\pi Z_{\text{eff}}(\alpha,Z)mc^2$, where an effective charge Z_{eff} is a function of both α and the atomic number of the nucleus Z. Here, we use $Z_{\text{eff}} = Z$, and assume any small differences between the present model and the Dirac equation are due to subtle effects not considered in the present model. Incorporating A12 into Eq. (V.4) gives

$$P_{sa} = \int_0^\infty \int_0^{\alpha\pi Z} \frac{4x^2\varepsilon^2}{2\pi}\left(1 - \frac{x^2\varepsilon^2}{3} + \cdots\right)\exp(-x)\frac{dx\,d\varepsilon}{4x^2\varepsilon^2\alpha\pi Z} = \frac{1}{2\pi} - \frac{\pi}{3}\frac{\alpha^2 Z^2}{3}. \tag{V.7}$$

This translates into a Z dependence of the geomagnetic ratio of hydrogen-like atoms of

$$g(1s)(\text{semiclassical}) = g_e\left[1 - \frac{\pi}{3}\frac{\alpha^2 Z^2}{3}\right]. \tag{V.8}$$

The standard Dirac equation based calculation of the corresponding quantity, to the same order, is [GRO70]

$$g(1s) = g_e\left[1 - \frac{\alpha^2 Z^2}{3}\right]. \tag{V.9}$$

For example, Eq. (V.9) predicts that the magnetic moment of an electron in a hydrogen atom differs from that of a free electron by -17750 ppb (parts per billion). The corresponding experimental value is $-17709(13)$ ppb [TIE77]. The small disagreement between Eq. (V.9) and experiment is due to higher-order and nuclear-mass correction terms [GRO70] not included here. The simple method presented here gives a $g(1s)$ $\alpha^2 Z^2$ coefficient that is 4.6% higher than the correct result [see Eq. (V.9)]. This comparison to the expectation from standard theoretical considerations partially justifies A7-A13, while highlighting a real difference for which we have no explanation at the present time.

VI. Exchange of virtual photons between a particle pair

For the exchange of photons between a pair of electrons, both the emission and absorption of the stimulated virtual photons, discussed previously, would be completely suppressed by energy conservation if only classical physics was assumed. We temporarily ignore this important fact and use the emission rate given by Eq. (II.2) and the reabsorption cross section of $\pi\lambda^2$ (for $\varepsilon < \varepsilon_R = \pi\hbar c/d$ as per A12) to calculate the repulsive force associated with the exchange of stimulated virtual photons between a pair of electrons

$$F = 2\int_0^{\varepsilon_R} \frac{d\varepsilon}{\pi\hbar}\frac{\varepsilon}{c}\frac{\pi\lambda^2}{4\pi d^2} = \frac{\hbar c}{2\pi d^2}\int_0^{\varepsilon_R}\frac{d\varepsilon}{\varepsilon}. \tag{VI.1}$$

The factor of two is because of the two-way exchange of the photons between an electron pair. The integral in Eq. (VI.1) is reminiscent of that used to obtain the Lamb shift is section III. There, we assumed that stimulated virtual emissions do not contribute to the smearing of an electron's location (A5), i.e. the stimulated virtual emission does not generate an observable recoil. We speculated that this was due to a lack of any symmetry-breaking in the single electron virtual-photon interaction. In the case of an exchange between a particle pair, spherical symmetry is broken by the presence of the partner electron. To obtain the force expressed by Eq. (VI.1) we have assumed the emission of the stimulated virtual photon generates a momentum change of the emitting particle (a recoil) of ε/c away from the absorbing partner, while the corresponding absorption generates a momentum change of the absorber particle of ε/c away from the emitter. A depiction of the virtual-photon exchange between a pair of electrons is presented in Fig. VI.1. The lack of a low-energy cutoff in Eq. (VI.1) leads to an infinite

force. To obtain a finite force strength, we need only include the low-energy cutoff associated with near-field effects, introduced in the previous section. If an attempted exchange were to be initiated, the reabsorption cross section would be reduced via the near-field effect discussed in section V, and given by Eq. (V.3). Perhaps less obvious, is that the cross section used to calculate the emission rate for initiating the exchange must also be multiplied by the error-function squared term from Eq. (V.3). This is due to time-symmetry arguments that apply equally to emission and absorption processes, i.e. in the case of a photon exchange between two electrons, the cross section for the stimulated emission (the emission rate) is influenced by the presence of the partner electron by the same factor that modifies the absorption cross section due to the presence of the partner. This is required because incident vacuum virtual photons with $\lambdabar \gg d$ cannot recognize the individual electrons in the pair, but instead see them as a collective object, and thus cannot generate stimulated virtual photons that cause the recoil of an individual electron, but cause the pair to recoil as a whole. The near-field effects considered here are analogous to the interaction properties of closely spaced classical antennas [IRA08].
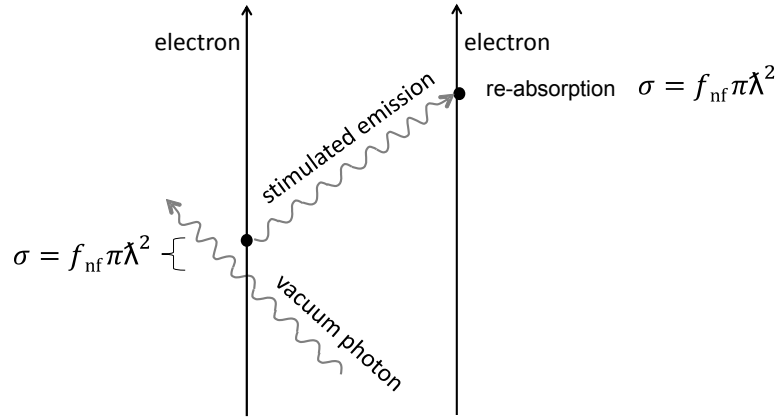

Fig. VI.1. Feynman-like diagram depicting the exchange of a virtual photon between an electron pair. This is almost the same as Fig. II.2 and Fig. V.3 except here the stimulated virtual photon terminates on the partner electron.

The reabsorption by the partner electron re-establishes conservation of energy and momentum but only after an exchange time of $t_{ex} = d/c$. As per A3 the probability that a stimulated virtual photon, is still in "existence" after a time t is given by $\exp(-t/\tau)$ with $\tau = \hbar/(2\varepsilon)$. Substituting in the exchange time gives a photon-exchange flux-reduction factor of $f = \exp(-\varepsilon/T_{ex})$ with an effective exchange temperature of $T_{ex} = \hbar c/(2d)$. In semi-classical treatments of photon emission [LES08] there is a factor of $1/(1-f)$ associated with the conversion of attempted classical escapes into real escapes. This modifies the exponential factor into the Planckian factor of $1/[\exp(\varepsilon/T)-1]$. For an electron pair without "surface effects" this factor can be partially justified by invoking:

  A13 The absorption of virtual photons by a partner electron generates a "time-reversed" virtual
       photon.

This is reminiscent of the stimulated emission of time-reversed photons with a probability of $\exp(-\varepsilon/T)$ following the absorption of an incident photon on a black hole [BEK77]. For a small black hole with a very high temperature, the stimulated emission probability of low-energy photons is unity. In the case of the exchange of virtual photons between an electron pair, perhaps the reabsorption of the first exchange generates a time-reversed virtual photon that retraces the path of the original exchange with a probability of making the jump back across the distance d, given by f (just as in the original exchange). This, in turn, generates an additional exchange with a further reduction of f, and so forth. The combined effect of

these multiple time-reversing exchanges gives a factor of $f + f^2 + f^3 + f^4 + \ldots = f/(1-f) = 1/[\exp(\varepsilon/T_{ex})-1]$. Assuming this factor applies, and including the near-field effects discussed above, the flux of virtual photons emitted from one electron, available for absorption by a partner (different) electron, per unit solid angle, is given by [see Eq. (II.2)]

$$f_{ex}(\lambda, d) = \frac{1}{4\pi} \int_0^{\varepsilon_R} \text{erf}^2\left(\frac{d}{\lambda\sqrt{2}}\right) \frac{1}{[\exp(\varepsilon/T_{ex})-1]} \frac{d\varepsilon}{\pi\hbar}. \tag{VI.2}$$

The corresponding force between two electrons is

$$F = 2\frac{1}{4\pi} \int_0^{\varepsilon_R = \pi\hbar c/d} \text{erf}^2\left(\frac{d}{\lambda\sqrt{2}}\right) \frac{1}{[\exp(\varepsilon/T_{ex})-1]} \frac{d\varepsilon}{\pi\hbar} \frac{\varepsilon}{c} \text{erf}^2\left(\frac{d}{\lambda\sqrt{2}}\right) \frac{\pi\lambda^2}{d^2}. \tag{VI.3}$$

Switching into energy in units of $T_{ex} = \hbar c/(2d)$ gives the more compact result

$$F = \frac{\hbar c}{2\pi d^2} \int_0^{2\pi} \frac{\text{erf}^4\left(\varepsilon/2^{3/2}\right)}{\varepsilon[\exp(\varepsilon)-1]} d\varepsilon, \tag{VI.4}$$

and thus an estimate of the fine-structure constant of

$$\alpha = \frac{1}{2\pi} \int_0^{2\pi} \frac{\text{erf}^4\left(\varepsilon/2^{3/2}\right)}{\varepsilon[\exp(\varepsilon)-1]} d\varepsilon = \frac{1}{139.713\ldots}, \tag{VI.5}$$

with a corresponding fundamental unit of charge of 1.587×10^{-19} C. This is incorrect by ~2%, or by a factor of ~2.7α. A difference of this size might be due to higher-order corrections not considered is this section.

It may appear as though there is an inconsistency between the use of the erf^4 term in Eq. (VI.4) and the erf^2 term in Eq. (V.4). In the calculation of the anomalous magnetic moment of the electron we use the erf^2 term to modify the reabsorption cross section, because the relevant photons have knowledge of both the birth and reabsorption locations, and thus the separation distance d. In the case of the anomalous magnetic moment, the initial stimulated emission is on a single isolated electron and we thus assume the unmodified cross section of $\pi\lambda^2$ ($\varepsilon < \varepsilon_H$). In the case of a photon exchange, both the emission and absorption events are aware of the location of the corresponding partner electron.

The force associated with the semi-classical exchange of virtual photons between two particles represented by Eq. (VI.4) can only generate repulsion. However, an attractive force between oppositely charged particles can be obtained by assuming the opposite charge is associated with a hole in a Fermi-sea of negative-energy particles [BJO64, chap. 5].

VI.1   Possible recoil corrections

If, in quantum field theory, one tries to obtain a simple result, there is often a series of higher-order corrections. However, if not following a traditional path, it can be difficult to assess the type of higher-order effect that should be included next. Here we are guided by the discrepancy between our calculated values of $(g-2)/2 = \alpha/(2\pi)$ and $\alpha^{-1} = 139.713$, and the corresponding experimental results. This is, of course, fraught with danger, given the simplistic methods used here to estimate the electron's anomalous magnetic moment and the fine-structure constant. For example, the discrepancy in the fine-structure-constant calculation might reflect the use of the sharp high-energy reabsorption cutoff used previously, and might have little to do with the recoil corrections proposed below. Ignoring the real possibility of adding confusion, we proceed with our analysis.

Assuming that a relatively simple correction factor can transform our calculated value of $\alpha^{-1} = 139.713$ into a value very close to the known experimental value, we write $\alpha^{-1} = 137.0359991 = 139.713/(1+a\alpha)^2$. The corresponding solution is $a = 1.332$. This is within 1-part per 1000 from 4/3,

which is reminiscent of the 4/3 factor in the recoil correction needed to obtain the Compton cross section in section IV. Similarly, we write $(g–2)/2 = 0.001159652 = \alpha/(2\pi) \times (1–ab\alpha)$. Assuming $a = 4/3$, the corresponding solution is $b = 0.156$, within ~2% of $1/(2\pi)$, and reminiscent of the stimulated virtual photon reabsorption probability used to estimate the anomalous magnetic moment of the free electron in section V. These results may be fortuitous. However, we proceed to explore the possibility of electron-recoil based corrections to our calculated estimates of α and $(g–2)/2$. Before doing this it is beneficial to revisit the explanation of the electron's rest mass given in section II.

As per section II, the rest-mass energy of a point particle is stored in the virtual-photon emissions stimulated by the passage of nearby vacuum virtual photons in the energy range from zero to $2\pi mc^2$. Each stimulated emission typically stores an energy of mc^2, these emissions are spaced in time by $\sim\hbar/(2mc^2)$, and each lasts for a time period of $\sim\hbar/(2mc^2)$. This is reminiscent of the Zitterbewegung obtained from the Dirac equation [BJO64, pg 38]. In the time period of $\sim\hbar/(2mc^2)$ the stimulated virtual photon and the massless naked electron both recoil a distance $\hbar c/(2mc^2) = \lambda_C/2$, giving an effective electron size of $\sim\lambda_C$ as depicted in Fig. VI.2 (a) (and as discussed in section II). However, this is an over simplistic view because the emissions are not uniformly spaced in time, and most, $1–1/(2\pi)$ of the stimulated emissions will temporarily store more than mc^2, which lives for a time scale less than $\hbar/(2mc^2)$. A better, but still crude, depiction of the electron is given in Fig. VI.2 (b). In this figure, there are six high-energy stimulated emissions ($\varepsilon > mc^2$) for the one low-energy stimulated emission ($\varepsilon < mc^2$). The rarer low-energy emissions can exist for a time scale much larger than the mean spacing between emission events, and are therefore usually followed by multiple high-energy stimulated emissions before the low-energy emission is terminated. The dotted line in Fig. VI.2 shows the naked-electron's trajectory if the low-energy emission was not followed by several high-energy stimulated emissions. The average trajectory of the recoil following the low-energy emission is shown by the dash-dotted line. The multiple high-energy emissions following the low-energy emission restrict the recoil of the naked-electron to distance of $\sim\lambda_C/2$. However, note that the low-energy stimulated virtual photons extend about one-half of their wavelength out from the center of the electron "cloud." This makes the exchange of low-energy stimulated virtual photons between an electron pair possible, as needed for the fine-structure-constant calculation presented in the previous subsection.

In section III the Compton cross section was obtained using A6 to calculate the probability that the absorption of a real photon of energy ε, generates a real photon of the same energy due to the acceleration associated with the recoil. In this case, the assumed recoil velocity and corresponding acceleration were $v = \varepsilon/(mc)$ and $a = 2\varepsilon^2/(\hbar mc)$, respectively. These quantities were estimated using the whole electron mass, m. For the case of virtual emissions due to the accelerations associated with the constant jiggling of the naked-electron as depicted in Fig. VI.2, we invoke:

A14 Virtual-photon emission associated with the acceleration of a "naked" electron can be determined as per A6, except with the recoil velocity replaced by c.

The corresponding effective acceleration over the absorption time of $t = \hbar/(2\varepsilon)$ is $a = 2c\varepsilon/\hbar$. Applying the same logic as done in section III gives a virtual-photon emission probability of $P = 4\alpha/3$ per stimulated virtual-photon recoil, independent of ε. This additional virtual-emission process increases the stimulated virtual-photon emission by a factor of $1+4\alpha/3$. As per the discussion in the previous subsection, time-symmetry arguments connect emission and absorption processes, and thus the emission enhancement must be mirrored by a corresponding enhancement on the absorption side of the photon exchange between an electron pair. These effects modify Eq. (VI.5) to

$$\alpha = \frac{(1 + 4\alpha/3)^2}{2\pi} \int_0^{2\pi} \frac{\mathrm{erf}^4(\varepsilon/2^{3/2})}{\varepsilon[\exp(\varepsilon) - 1]} d\varepsilon = \frac{(1 + 4\alpha/3)^2}{139.713}. \tag{VI.6}$$
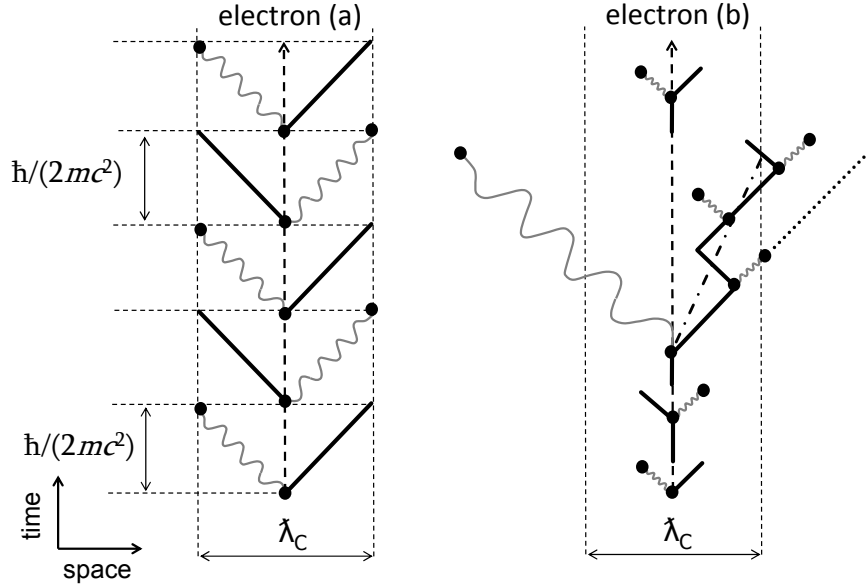
Fig. VI.2. An extension of Fig. II.2, showing the repeated stimulated virtual-photon emissions responsible for the electron's rest mass (see text). The stimulating vacuum virtual photons are not shown. (a) Depicts a simple representation where the stimulating vacuum virtual-photon energy is always mc^2 with the corresponding stimulations equally spaced in time. (b) An attempt to represent one of the complications associated with the spread in the stimulating vacuum photon energies (see text).

The corresponding solution is $\alpha^{-1} = 137.03(2)$. The uncertainty of $\Delta(\alpha^{-1}) = \pm 0.02$ was assessed by assuming a recoil-correction factor of $(1+4\alpha/3\pm\alpha^2)^2$, and should only be used as a rough guide. The corresponding charge is $1.6022(1) \times 10^{-19}$ C. The reader is reminded that Eq. (VI.6) is not based on first principle expectations from a deep knowledge of QED but rather a plausibility argument in an attempt to rectify the discrepancy between Eq. (VI.5) and the known experimental result. Without detailed calculations to justify the recoil-correction factor, a healthy dose of skepticism should be applied.

In a similar fashion, as above, we now attempt to reverse-engineer a simple "rule" that gives the discrepancy between the calculated second-order $(g–2)/2 = \alpha/(2\pi)$ and the corresponding experimental value of 0.001159652. An assumption that can be used to obtain the desired result is:

A15 A7-A11 still apply, except the one Bohr magneton is only generated if the recoil-induced photon is not generated or "terminates" in free space (i.e. it is not re-absorbed).

We have no plausibility argument for A15 other than invoking it gives the desired results. The relevant Feynman-like diagrams are shown in Fig. VI.3. The diagram on the left is the same as Fig. V.1, except the recoil after the stimulated emission is depicted, even though this diagram does not contain an additional recoil-induced virtual photon. This diagram is associated with a probability of $(1–4\alpha/3)$ because this is the probability of not generating the additional recoil-induced virtual photon. The diagram on the right is associated with a probability of $4\alpha/3$ (see discussion above). The probability associated with the left diagram is multiplied by the α term associated with the absorption cross section and the probability of reabsorption, $1/(2\pi)$ (see section V), to obtain its contribution to $(g–2)/2$ (see Fig. VI.3). The probability associated with the right diagram is also multiplied by the same factors, but with the additional probability that the virtual-photon associated with the recoil is not absorbed, $1–1/(2\pi)$. We have assumed these probabilities are unaffected by the emission and/or possible reabsorption of the

other photon. Additional higher-order effects are likely to modify these probabilities slightly. The anomalous magnetic moment associated with the combined effect of both diagrams in Fig. VI.3 is

$$\frac{(g-2)}{2} = \frac{\alpha}{2\pi}\left(1 - \frac{4\alpha}{3 \cdot 2\pi}\right). \tag{VI.7}$$

The corresponding numerical value is $(g-2)/2 = 0.0011591(6)$. The fourth-order correction factor of $[1-4\alpha/(6\pi)]$ differs from standard QED by a relative factor of $\sim(1+2\alpha)$. The uncertainty of $= \pm0.0000006$ was assessed by assuming a recoil-correction factor of $1-4\alpha/(6\pi)\pm\alpha^2$, and should only be used as a rough guide. The reader is reminded that Eq. (VI.7) is not based on a first principles expectation from a deep knowledge of QED but rather a plausibility argument in an attempt to find a simple fourth-order correction that gives a result close to the known experimental result. A healthy dose of skepticism should be applied.
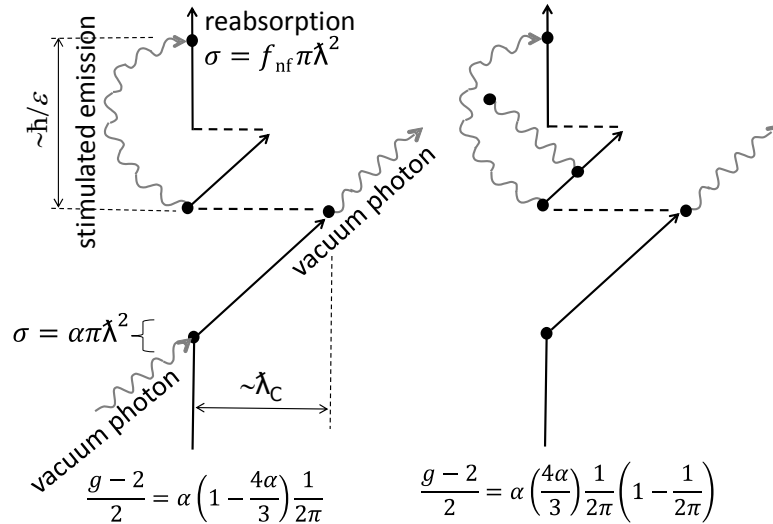

Fig. VI.3. Two Feynman-like diagrams associated with the anomalous magnetic moment of the free electron, including recoil effects.

VII.   Summary and conclusions

By assuming that vacuum virtual photons can stimulate an isolated electron to emit additional virtual photons with a cross section of $\pi\lambda^2$, and invoking a high-energy cutoff of $2\pi mc^2$, beyond which virtual photons no longer interact with a particle of mass m; the additional average energy associated with the cloud of stimulated virtual photons surrounding a particle is equal to the particle's rest-mass energy, mc^2. This storage of the rest-mass energy in the surrounding cloud of virtual photons is similar to the storage of the rest-mass in the surrounding classical electric field, but without of the infinity associated with point particles. The high-energy cutoff of $2\pi mc^2$, in conjunction with the low-energy Lamb shift cutoff suggested here, and an absorption/recoil/re-emission "doorway" cross section of $\alpha\pi\lambda^2$, leads to a calculated hydrogen Lamb shift of 1058 MHz, in agreement with experiment. Additional support for a QED "doorway" cross section proportional to $\pi\lambda^2$ is obtained via a semi-classical picture of Compton scattering. The inclusion of semi-classical near-field effects and other model choices give the anomalous magnetic moment of the free electron. These choices are partially justified by their ability to also give an atomic number dependence of the anomalous magnetic moment of electrons in hydrogen-like atoms near the standard QED result.

An expression for the fine-structure constant can be obtained if electromagnetism is assumed to be associated with the exchange of stimulated virtual photons between particle pairs. Our first semi-classical estimate of the repulsive force generated by the exchange of virtual photons between a pair of particles, obtained using only the far-field interaction cross section of $\pi\lambdabar^2$, is infinite. Including an estimate of near-field effects leads to a force that defines a fundamental unit of charge of $\sim 1.6\times10^{-19}$ C. The difference from the known value might be due to recoil effects, perhaps as speculated in section VI. By including these speculative effects, an inverse fine-structure constant of $\alpha^{-1}=137.03(2)$ and a corresponding calculated charge of $1.6022(1)\times10^{-19}$ C are obtained. We feel that we cannot currently dismiss the possibility that the fine-structure constant is obtainable via a far-field emission/absorption cross section of $\pi\lambdabar^2$ with near-field and recoil corrections. A summary of our reverse-engineered semi-classical results is presented in Table VII.1.

Table VII.1. Summary of the semi-classical results obtained here, and a comparison with QED.

Observable	Simple reverse-engineered results		QED
	Reason	Formula	
Lamb shift (excluding vacuum polarization)	Absorption and re-emission of vacuum virtual photons	$\Delta E_{2s} = \dfrac{\alpha^5 \ln(2\pi^2/\alpha)}{6\pi} mc^2$ $= 1072$ MHz	$= 1072$ MHz
Compton scattering	Absorption, recoil, and re-emission of the incident photon	$\sigma = \alpha\pi\lambdabar^2 \dfrac{4\alpha}{3} \dfrac{\varepsilon^2}{(mc^2)^2} 2$ $= 8\pi(\alpha\lambdabar_C)^2/3$	$= 8\pi(\alpha\lambdabar_C)^2/3$
Anomalous magnetic moment of the free electron	Stimulated emission and reabsorption including near-field and recoil effects, following the absorption and re-emission of vacuum virtual photons	$\dfrac{(g-2)}{2} = \dfrac{\alpha}{2\pi}(1 - \dfrac{4\alpha}{3}\dfrac{1}{2\pi})$	$= \dfrac{\alpha}{2\pi}\left(1 - 0.985\ldots\dfrac{4\alpha}{3}\dfrac{1}{2\pi}\right)$
Magnetic moment of the electron in hydrogen-like atoms	Stimulated emission and reabsorption including near-field effects	$g(1s) = g_e(1 - \dfrac{\pi}{3}\dfrac{\alpha^2 Z^2}{3})$	$= g_e(1 - \dfrac{\alpha^2 Z^2}{3})$
Fine-structure constant	Exchange of stimulated virtual photons including near-field and recoil effects	$\alpha = \dfrac{(1 + 4\alpha/3)^2}{2\pi}\displaystyle\int_0^{2\pi} \dfrac{\mathrm{erf}^4(\varepsilon/2^{3/2})}{\varepsilon[\exp(\varepsilon)-1]}d\varepsilon$ $=1/(137.03)$	137.0359991 (experiment)

Additional work on photon-particle near-field corrections and recoil effects is needed. If the semi-classical choices made here can be justified by detailed calculations, then an understanding of the numerical value of the fine-structure constant may emerge. Despite the speculative nature of several of the arguments used to obtain a calculated value near to the known fine-structure constant, the present study suggests that charge is an emergent property generated by a simple interaction mechanism between point-like particles and the electromagnetic vacuum, similar to the mechanisms that generate the Lamb shift and the anomalous magnetic moment of the electron.

References

[AOY07] T. Aoyama, M. Hayakawa, T. Kinoshita, and M. Nio, Phys. Rev. Lett. **99**, 110406 (2007).
[AOY12] T. Aoyama, M. Hayakawa, T. Kinoshita, and M. Nio, Phys. Rev. D **85**, 033007 (2012).
[BEK77] J. D. Bekenstein and A. Meisels, Phys. Rev. **D 15**, 2775 (1977).
[BET47] H. A. Bethe, Phys. Rev. **72**, 339 (1947).
[BET50] H. A. Bethe, L. M. Brown, and J. R. Stehn, Phys. Rev. **77**, 370 (1950).
[BJO64] J. D. Bjorken and S. D. Drell, Relativistic Quantum Mechanics,
         McGraw-Hill ISBN 07-005493-2 (1964).
[DIR27] P. A. M. Dirac, Proc. Roy. Soc. (London) **A114**, 243 (1927), **A117**, 610 (1928).
[DYS49] F. Dyson, Phys. Rev. **75**, 486 (1949), **75**, 1736 (1949).
[FEY49] R. P. Feynman, Phys. Rev. **76**, 749 (1949), **76**, 769 (1949).
[GAB06] G. Gabrielse, D. Hanneke, T. Kinoshita, M. Nio, and B. Odom, Phys. Rev. Lett. **97**, 030802
         (2006) and **99**, 039902 (2007).
[GRO70] H. Grotch, Phys. Rev. Lett. **24**, 39 (1970).
[HAN56] R. Hanbury Brown and R. Q. Twiss, Nature **177**, 27 (1956), and
         R. Hanbury Brown and R. Q. Twiss, Nature **178**, 1046 (1956).
[IRA08] Z. Irahharten et al., IEEE International Conference on Communication, 2008, pg. 4872.
[JAC75] J. D. Jackson, Classical Electrodynamics, John Wiley & Sons, Inc. (1975).
[KAR52] R. Karplus, A. Klein, and J. Schwinger, Phys. Rev. **86**, 288 (1952).
[KAR98] S. G. Karshenboim, Can. J. Phys. **76**, 168 (1998).
[KEM33] E. C. Kemble and R. D. Present, Phys. Rev. **44**, 1031 (1933).
[KIN06] T. Kinoshita and M. Nio, Phys. Rev. D **73**, 013003 (2006).
[LAM47] W. E. Lamb and R. C. Retherford, Phys. Rev. **72**, 241 (1947).
[LAP96] S. Laporta and E. Remiddi, Phys. Lett. B, **379**, 283 (1996).
[LES08] J. P. Lestone, Mod. Phys. Lett. A, **23**, 1067 (2008).
[MOH15] P. J. Mohr et al, http:/physics.nist.gov/constants (2015), National Institute of Standards and
         Technology, Gaithersburg, MD 20899, USA.
[PET57] A. Petermann, Helv. Phys. Acta, **30**, 407 (1957).
[SCH48] J. Schwinger, Phys. Rev. **73**, 416 (1948), **74**, 1439 (1949), **76**, 790 (1949).
[TIE77] J. S. Tiedeman and H. G. Robinson, Phys. Rev. Lett. **39**, 602 (1977).
[TOM46] S. Tomonaga, Prog. Theor. Phys. **1**, 27 (1946).
[UEH35] E. A. Uehling, Phys. Rev. **48**, 55 (1935).
[WEL48] T. A. Welton, Phys. Rev. **74**, 1157 (1948).